

Crushable Finite Element Modeling of Mechanical Properties of Titanium Foam

Nada S. Korim¹, Mohammed Y. Abdellah^{2,3}, Montasser Dewidar¹, Ayman M.M. Abdelhaleem⁴

¹Department of materials and Mechanical engineering, Faculty of Energy Engineering, Aswan University, Aswan, Egypt

²Production Engineering and Mechanical Design, South Valley University, Qena, 83523, Egypt

³Mechanical Engineering Department, Collage of Engineering and Islamic Architecture, Umm Al-Qura University Makkah, KSA

⁴Mech. Design and Prod. Eng. Dep., Faculty of Engineering, Zagazig University, Zagazig, Egypt

Abstract— Titanium foam is attractive material in bio-system applications, due to its biocompatibility as well as stable fixation in human bone. Obtaining sufficient information about mechanical and failure behaviors of such material are of great intense and it needs to be will studied. Finite element model based on crushable foam model will be used to simulate the mechanical and failure behavior of titanium foam of vary densities as 59.9 %, 62.5 % and 65 % porosity. Compression test is commonly test for foam material to measure compressive strength and flow behaviors of titanium foam with pervious porosity. Whereas, stiffness properties to be measured three point bending test is getting good. The three point bending test is used to measure both flexural strength and flexural stiffness or young modulus. The numerical modeling results are validated with other available published. The results are in good agreement with the published experimental data.

Index Terms— Titanium foam, porosity, finite element analysis, crushable foam model, bio-system, compression test, the three point bending test.

INTRODUCTION

Metal foams are new materials, which have many applications as in automotive structural components, aircraft and spacecraft structures, shock absorbers, sound and vibration dampeners, biomedical implants and heat exchangers [1], [2], [3]. Metal foam is very important because it have many properties such as low density, high specific stiffness, good energy absorption capability and high specific strength [4], [5].

Titanium foams are favored in many applications including biomedical implants where biocompatibility is required. The main reason for using foam metals is the increase of the friction coefficient between the implant and the surrounding bone. Mechanical interlocking of bone with the implant is allowed by substantial bone in-growth and better long-term stability. Moreover, stiffness of the implants can be increased by varying porosity to reduce the stress shielding effect [5], [6]. One of auspicious biomedical application of Tifoams is in dental implant. Finite element analysis is used for designing of dental implants and the success of the use of finite element method depend on analyzing structures and components rests upon the accuracy and efficiency of the applied material models [7], [8], [9], [10], [11].

Tanwongwan and Carmai [12] construct finite element model to simulate the compression and flexural strength of titanium foam with varying densities, the simulation was in good agreement with the experimental results while the description of plasticity are not completely explain.

Other constitutive models [13], [14], [15], [16] had been implemented in finite element commercial code to simulate met-

al foam in general and aluminum and Ti- ones in especial case.

The main goal of the present paper is to simulate the flow behavior of titanium foam under both compression and bending load using crushable foam model implemented in finite element subroutine. The model description is completely detailed in this paper.

MECHANICAL BEHAVIORS OF METAL FOAMS

Foam microstructure is the major difference between foam materials and solid materials.

Cells or pores, which are present in metal foams, can be considered as sponge. Metal foams can be characterized at microstructure level by relative density, cell topology, cell shape and cell size [17], [18], [19]. The porosity is a parameter, which is used to indicate the proportion of porous area in foams.

These microstructure features are affecting the mechanical responses of metal foams. The compressive stress-strain curve for a metal foam is specified by three zones; one of these zones is a linear elastic zone, which is corresponding to cell bending or face stretching. The second one is a stress plateau zone that is corresponding to progressive cell failure by plastic yielding or elastic buckling. In addition, the last zone is the densification zone, which is corresponding to failure of the cell throughout the material and subsequent loading of cell edges and faces against one. Metal foam of low relative density can be deformed up to large strain before densification occurs [20]. Complete information and investigation for the plastic yield

surface and subsequent plastic flow behavior of a metal foam is very essential and important. Metal foams can yield under hydrostatic loading moreover to deviatoric loading in contrast to solid metals [4].

ELASTIC AND CRUSHABLE MODEL

The mechanical behavior of Ti-foam will be employed by isotropic elasticity and isotropic crushable foam hardening plasticity. The simplest form of linear elasticity is the isotropic case, and the stress-strain relationship is given the following strain tensors Eqn. [21].

$$\begin{pmatrix} \varepsilon_{11} \\ \varepsilon_{22} \\ \varepsilon_{33} \\ \gamma_{12} \\ \gamma_{13} \\ \gamma_{23} \end{pmatrix} = \begin{bmatrix} 1/E & -\nu/E & -\nu/E & 0 & 0 & 0 \\ -\nu/E & 1/E & -\nu/E & 0 & 0 & 0 \\ -\nu/E & -\nu/E & 1/E & 0 & 0 & 0 \\ 0 & 0 & 0 & 1/G & 0 & 0 \\ 0 & 0 & 0 & 0 & 1/G & 0 \\ 0 & 0 & 0 & 0 & 0 & 1/G \end{bmatrix} \begin{pmatrix} \sigma_{11} \\ \sigma_{22} \\ \sigma_{33} \\ \sigma_{12} \\ \sigma_{13} \\ \sigma_{23} \end{pmatrix}$$

The elastic properties are completely defined by giving the Young's modulus E, and the Poisson's ratio ν . The shear modulus G, can be expressed in terms of E and ν as

$$G = \frac{E}{2(1+\nu)} \tag{1}$$

The use of crushable foam plastic model is to model the enhanced ability of a foam material to deform in compression due to cell wall buckling processes (it is assumed that the resulting deformation is not recoverable instantaneously and can, thus, be idealized as being plastic for short duration events).

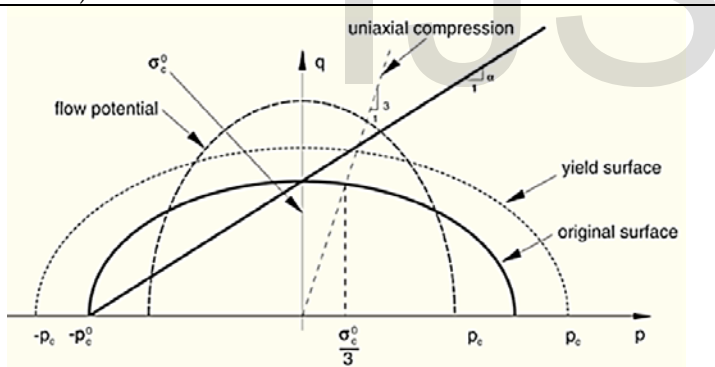


Fig (1) Crushable foam model with isotropic hardening: yield surface and flow potential in the p-q stress plane [22]

Crushable foam model with isotropic hardening uses a yield surface that is an ellipse centered at the origin in the p-q stress plane [22].

$$F = \sqrt{q^2 + \alpha^2 p^2} - B \tag{2}$$

Where F is a yield surface for the isotropic hardening model, p is the pressure stress, q is the Mises stress and B is the size of the (vertical) q-axis of the yield ellipse that obtained from equation (3)

$$B = \alpha p_c = \sigma_c \sqrt{1 + \left(\frac{\alpha}{3}\right)^2} \tag{3}$$

Where α is the shape factor of the yield ellipse that defines the relative magnitude of the axes, p_c is the yield stress in hydrostatic compression, and σ_c is the absolute value of the yield stress in uniaxial compression, and α is the shape factor that can be computed using the initial yield stress in uniaxial compression is given from

$$\alpha = \frac{3k}{\sqrt{9-k^2}} \tag{4}$$

The flow potential for the isotropic hardening model is chosen as v_p

$$G = \sqrt{q^2 + \beta^2 p^2} \tag{5}$$

$$\beta = \frac{3}{\sqrt{2}} \sqrt{\frac{1-2v_p}{1+v_p}} \tag{6}$$

Where v_p is the plastic Poisson's ratio given by

$$v_p = \frac{3-k^2}{6} \tag{7}$$

COMPRESSION TEST

The elastic properties are completely defined by giving the Young's modulus, E, the plastic Poisson's ratio, v_p , and the compressible stress ratio (k). The Young modulus (E) of different porosity Ti-foam was calculated using equation (8) which obtained from the experiments of Imwinkelried [13].

$$E = E_s (-0.024 + 15.86 \rho_r^2) \tag{8}$$

Where (E_s) is the Young's modulus of the fully solid titanium, which is taken as 110 Pa for pure titanium [13] and ρ_r is relative density of the metal foam. In Imwinkelried experimental data, the relative density is linearly proportional to percent of porosity.

According to shape of the specimen, the plastic Poisson's ratio (v_p) was assumed 0.34 but the compressible stress ratio (k) was calculated as 0.98 from equation (7)

THREE POINT BENDING TEST

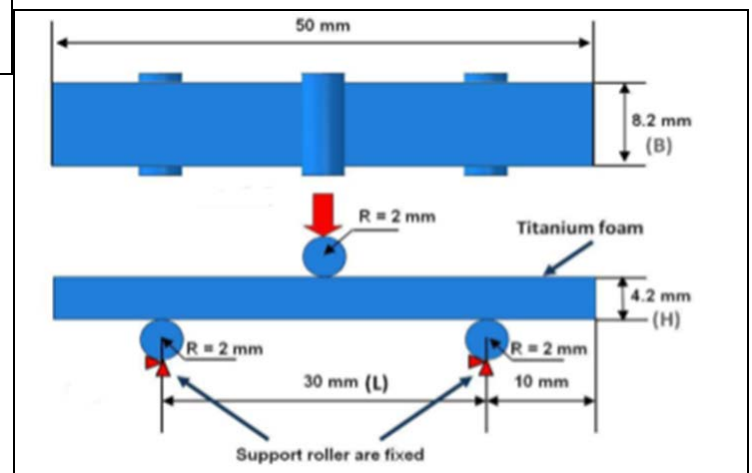


Fig (2) three point bending test

The maximum bending stress was calculated using equation 9

$$\sigma_{bending} = \frac{3FL}{2BH^2} \quad (9)$$

In this paper, flexural strength and flexural stiffness have been inference

$$E = \frac{FL^3}{48 I_f \rho_r^{1.5}} \quad (10)$$

Where L is the free length between the supports; F, the measured force; f, the displacement of the plunger; and $I = BH^3/12$, the moment of inertia with height H and width B.

$$\sigma_f = \frac{\sigma_c}{4.12 \rho_r^{-0.236}} \quad (11)$$

Where σ_c is the compressive strength of Ti-foam (MPa); σ_f is the flexural strength of Ti-foam (MPa).

FINITE ELEMENT DOMAIN AND MESHING

A) THE COMPRESSION DOMAIN:

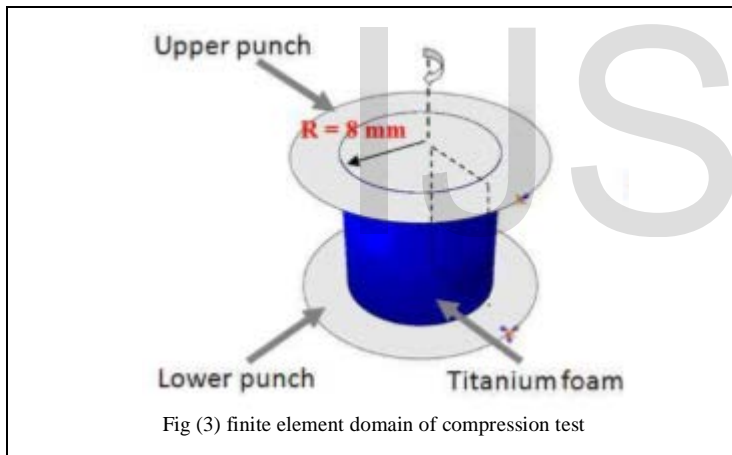


Fig (3) finite element domain of compression test

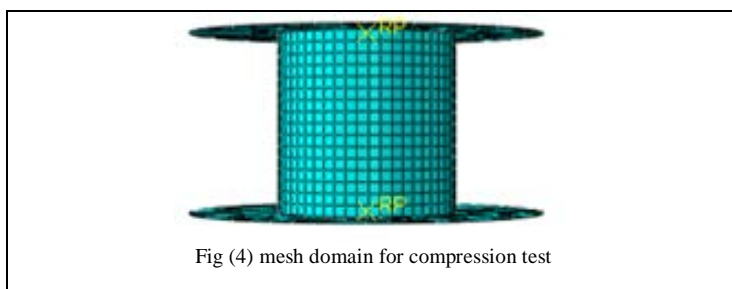


Fig (4) mesh domain for compression test

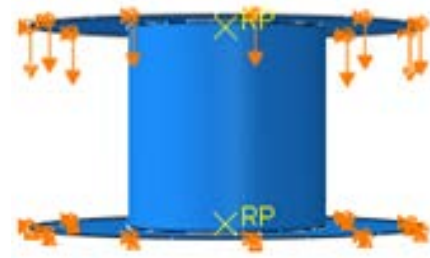


Fig (5) boundary condition for compression test

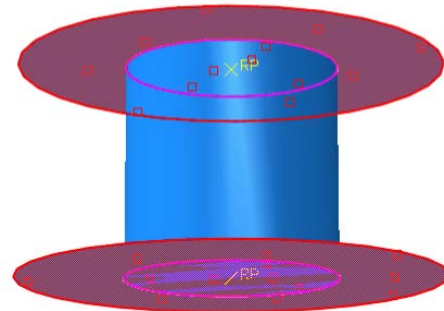


Fig (6) interaction module between Ti-foam cylinder and the upper and the lower die

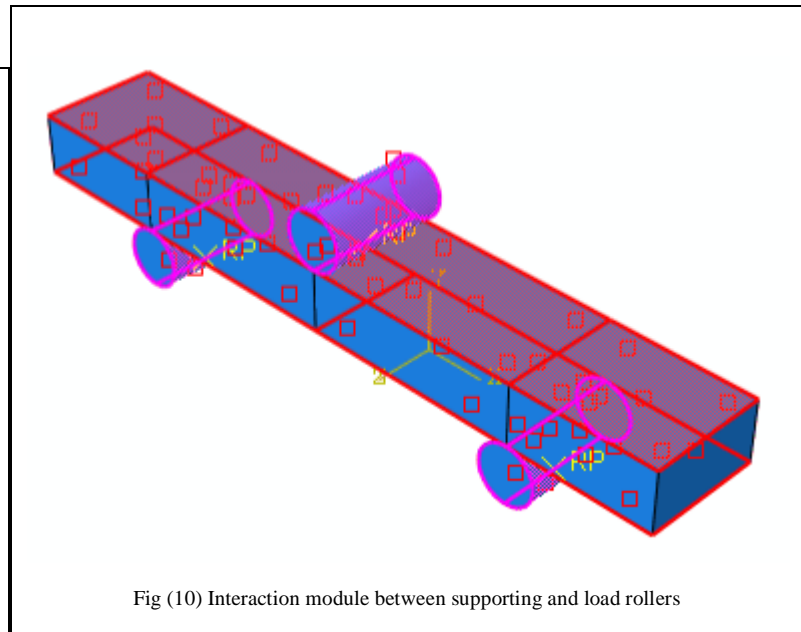
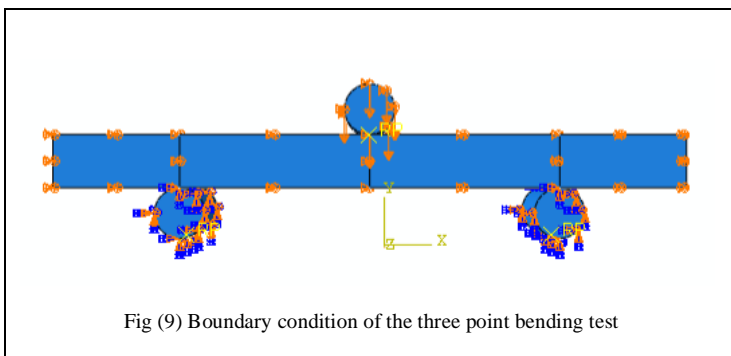
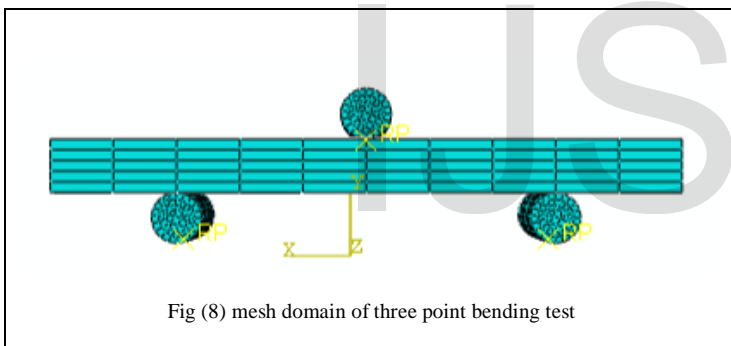
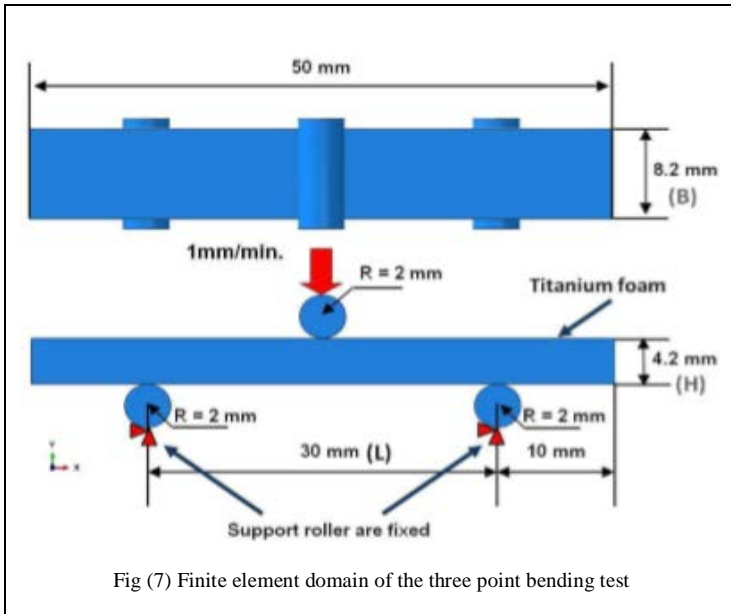
A compression test of Ti-foam cylinder with 8mm diameter and 16mm height as shown figure (3) was simulated to test the crushable foam model in describing the mechanical behavior of the Ti-foam. The upper flat die is loaded by 5N while lower flat die was fixed. C3D8R: An 8-node linear brick, reduced integration and hourglass control are used. The friction coefficient between the contact surfaces was set to be 0.5 [21]. The mechanical properties of Ti-foam for compression test are taken from crushable and compressive equations, which are listed in table 1.

Table 1 The mechanical properties of Ti-foam for compression test are measured from crushable and compressive per-vious model.

	Porous 62.5%	Porous 59.9%	Porous 65%
Young's modulus, E (MPa)	242700	277900	211000
Poisson's ratio, v	0.3	0.3	0.3
Compression yield stress ratio, k	0.98	0.98	0.98
Plastic poisson's ratio, v_p	0.34	0.34	0.34

The upper and lower platen of the compression die are assembled by interaction module and are given other properties. Fig (3) shows finite element domain and Fig (4) shows mesh domain of Ti-foam. Fig (5) shows boundary condition for compression test and Fig (6) interaction module of Ti-foam.

B) THE THREE POINT BENDING DOMAIN



The three point bending test of Ti-foam was simulated by the same material module as used in compression test. Finite element domain of three dimensional of three point bending test was constructed as shown in figure (7). The upper movable roller was loaded by 1N while the lower rollers were fixed. C3D8R: An 8-node linear brick, reduced integration, hourglass controls are used. The friction coefficient between the contact surfaces was set to be 0.5 [21]. The mechanical properties of Ti-foam specimen for three point bending test are taken from crushable and three point bending equations, which are listed in table 2 while the mechanical properties of the upper and lower roller are listed in table 3. Fig (7) Finite element domain of the three point bending test, Fig (8) mesh domain of three point bending test, Fig (9) Boundary condition of the three point bending test and Interaction module between supporting and load rollers is shown in Fig. (10).

Table 2 mechanical properties of Ti-foam specimen with porosity (62.5%, 59.9% and 65%) for three point bending test are measured from crushable and it's pervious model.

	Porous 62.5%	Porous 59.9%	Porous 65%
Young's modulus, E (MPa)	31893.3	35267	28757.7
Poisson's ratio, v	0.3	0.3	0.3
Compression yield stress ratio, k	0.98	0.98	0.98
Plastic Poisson's ratio, vp	0.34	0.34	0.34

Table 3 mechanical properties of the upper and lower roller with porosity (62.5%, 59.9%, 65%)

	Porous 62.5%	Porous 59.9%	Porous 65%
Young's modulus, E (MPa)	31893.3	35267	28757.7
Poisson's ratio, ν	0.3	0.3	0.3

The stress-strain curve obtained from the simulation is compared with experimental results [12] as shown in Fig. (11) For Ti-foam with (59.9%, 62.5%, and 65%) porosity. At the stress plateau regions, the results are in good agreement with the experimental ones. While the deviation at higher strain return to that plasticity has damage criteria, moreover failure criteria, which does not, implement in the model. When the displacement is increasing, the specimen starts to plastically deform under the compression where the maximum of compressive and tensile stresses is encountered. However, the softening in the experimental work is observed because the model does not take into account the damage or failure criteria.

RESULTS AND DISCUSSION

A) FOR THE COMPRESSION TEST

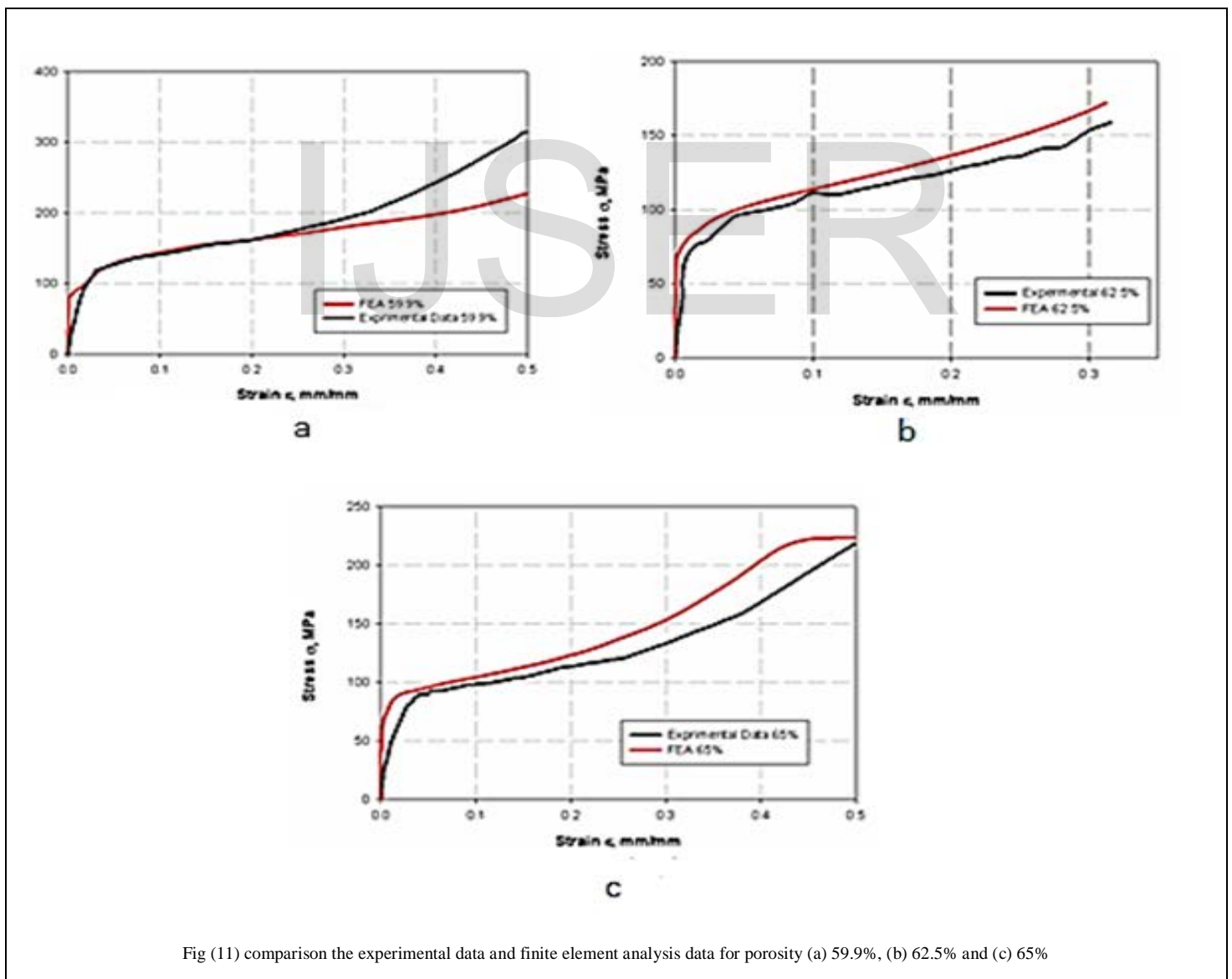
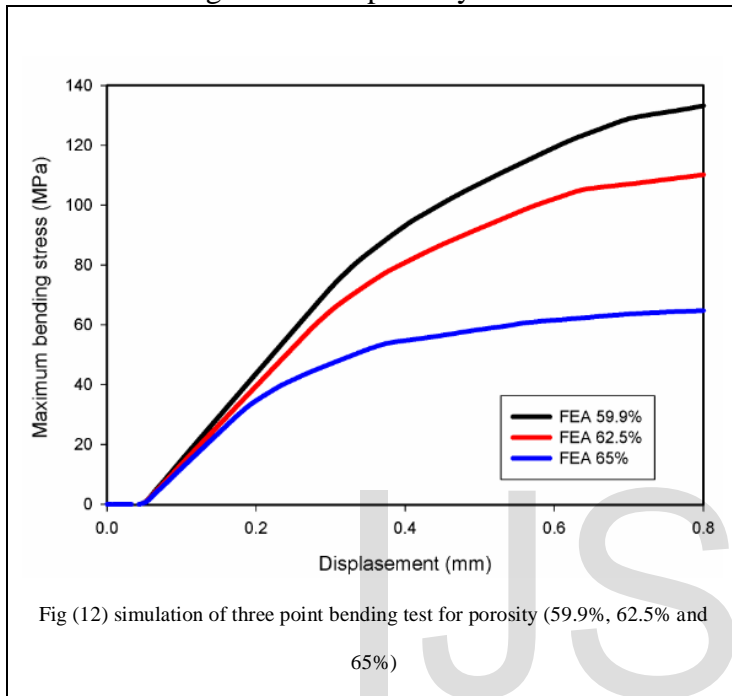


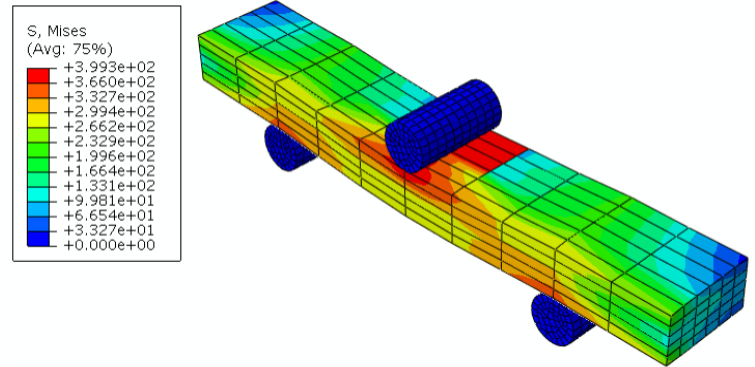
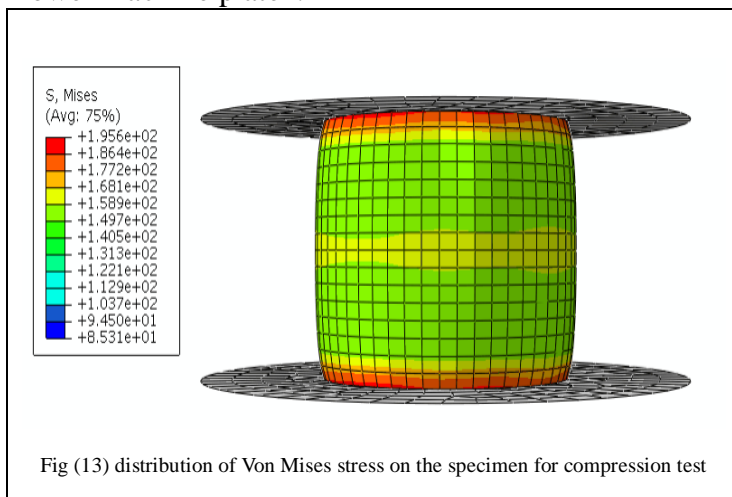
Fig (11) comparison the experimental data and finite element analysis data for porosity (a) 59.9%, (b) 62.5% and (c) 65%

B) FOR THREE POINT BENDING TEST

Typical bending stress–displacement curves for the three point bending tests are shown in Fig. 12. The bending stress strongly depends on the porosity of the titanium foam sample. It is illustrated that as porosity increase flexural strength decrease this is due to decrease of strength with the porosity increment.



The stress distribution and the failure modes are shown in contour image, which are shown in Fig. (13 and 14). It is clear that stress are very high at upper and lower surfaces at interfaces between upper and lower machine platen.



CONCLUSION

The use of crushable finite element analysis of titanium foam is proven to be good failure criteria to describe its mechanical properties with various porosity levels as (59.9%, 62.5% and 65% porosity) under compressive and bending loads. The obtained results for compression tests are in good agreement with the experimental ones whereas; the bending results deviate at higher displacement. The model can be used to measured bio-system based on Ti-foam material with great amount of accuracy.

REFERENCES

- [1] L.J. Vendra and A. Rabiei, "Evaluation of modulus of elasticity of composite metal foams by experimental and numerical techniques," *Mat. Sci. Eng. Vol 527*, pp. 1784-1790, 2007.
- [2] N. Tuncer and G. Arslan, "Designing compressive properties of titanium foams." *J. Mater. Sci.* vol 44 1477-1484, 2009.
- [3] J. Banhart, "Manufacture characterisation and application of cellular metals and metal foams." *Progress in Materials Science*, pp. 559- 632, 2001.
- [4] M.F. Ashby, A.G. Evan, N.A. Fleck, L.J. Gibson, J.W. Hutchinson, H.N.G. Wadley, *Metal Foams: A Design Guide*. London: Butterworth-Heinemann, 2000.
- [5] M.I. Z. Ridzwan and S. Shuib, "Problem of stress shielding and improvement to the hip implant designs." *J. Med. Sci.* vol 4, pp.460-467, 2007.
- [6] W. Yan and C.L. Pun, "Spherical indentation of metallic foams," *Mater. Sci. Eng. A*, vol 527, pp. 3166-3175, 2010.
- [7] A. Merdji, B. Bouiadjra, T. Achour, B. Seier, B. O. Chikh, and Z.O.Feng, "Stress analysis in dental prosthesis," *Com. Mater. Sci.*, vol 49, pp.126-133, 2010.
- [8] J. Yang and HJ. Xiang, "A three-dimensional finite element study on the biomechanical behaviour of an FGBM dental implant in surrounding bone," *J. Biomech.*, vol 40, pp.2377-2385, 2007.

- [9] O. Kayabasi, E. Yuzbasioglu, and F. Erzincanli, "Static, dynamic and fatigue behaviors of dental implant using finite element method," *Adv. Eng. Soft. Vol 37*, pp.649-658, 2006.
- [10] N. Djebbar, B. Serier, B. B. Bouiadjra, S. Benbarek, and A. Draï, "Analysis of the effect of load direction on the stress distribution in the dental implant," *Mater. Des. Vol 31*, pp. 2097-2101, 2010.
- [11] H. Schiefer, M. Bram, H.P. Buchkremer, and D. Stover, "Mechanical examinations on dental implants with porous titanium coating," *J. Mater. Sci: Mater. Med.*, vol 20, pp. 1763-1770, 2009.
- [12] W.Tanwongwan, J.Carmai "Finite Element Modeling of Titanium Foam Behavior for Dental Application" *Proceedings of the World Congress on Engineering 2011 Vol III WCE 2011*, July 6 -8, 2011, London, U
- [13] T. Imwinkelried, T. "Mechanical properties of open-pore titanium foam," *J. Biomed Mater Res A*, pp. 964-970, 2007.
- [14] S. Kashaf, A. Asgari, T. B. Hilditch, W. Yan, V. K. Goel, and P. Hodgson, "Fracture toughness of titanium foams for medical applications," *Mater. Sci. Eng. A*, vol 527, pp. 7689-7693, 2010.
- [15] H.L. Schreyer, Q.H Zuo, A.K Maji, "Anisotropic plasticity model for foams and honeycombs" *J. Eng. Mech.* pp. 1913-1930, 1994.
- [16] R. Miller, "A continuum plasticity model of the constitutive and indentation behavior of foamed metals," *Inter. J. Mech. Sci.* pp. 729-754, 1999.
- [17] A. Nouri, A.B. Chen, P.D. Hodgson, and C.E. Wen, "Preparation and characterization of New Titanium Based Alloys for Orthopaedic and Dental applications," *Adv. Mater. Res.*, vol 15-17, pp.71-76, 2007.
- [18] J. Bin, W. Zejun, and Z. Naiqin, "Effect of pore size and relative density on the mechanical properties of open cell aluminium foams," *Scripta. Mater. Vol 56*, pp.169-172, 2007.
- [19] A.-F. Bastawros, H. Bart-Smith, and A.G. Evans, "Experimental analysis of deformation mechanisms in a closed-cell aluminum alloy foam," *J. Mech. Phys. Solids.*, vol 48, pp.301-322, 2000.
- [20] L.J. Gibson and M.F. Ashby. *Cellular Solids: Structure and Properties*. 2nd ed. 1997, Cambridge University Press.
- [21] Obert, R. et al. *Frictional Properties of BIOFOAM™ Porous Titanium Foam*. Wright Medical Technology, 5677 Airline Rd, Arlington, TN 38002.
- [22] ABAQUS 6.9 help